
ARTICLE

Molecular Dynamics Study on Grain Boundary Diffusion of Actinides and Oxygen in Oxide Fuels

Masahiro NISHINA^{1,*}, Keita YOSHIDA¹, Tatsumi ARIMA¹
Yaohiro INAGAKI¹, Kazuya IDEMITSU¹ and Isamu SATO²

¹ Kyushu University, 744 Motooka, Nishi-ku, Fukuoka-shi, Fukuoka-ken, 819-0395, Japan

² Japan Atomic Energy Agency, 4002 Narita, Oarai, Higashi Ibaraki-gun, Ibaraki-ken, 311-1393, Japan

Diffusion phenomena of actinides and oxygen are relating to various properties of oxide fuels, e.g. actinide and oxygen redistribution, pore migration, sintering behavior. Although lots of experimental data have been obtained for U and O diffusions, these seem to be a little scattered among experiments. In addition, there are few studies of transuranium elements. Recently, we experimentally showed that diffusion coefficients of Am and Pu were almost comparable with that of U and the contribution of grain boundaries (GB) were relatively large in oxide fuels. On the other hand, the molecular dynamics (MD) calculation showed that U ions migrated via its vacancies and the O diffusion mechanism changed with temperature in bulk. In this study, the GB diffusion coefficients and the mechanism were systematically evaluated for U, Am and O in oxide fuels by MD calculations. For actinides and oxygen, their GB diffusion coefficients are significantly larger than bulk ones, and the diffusion mechanisms in GBs are almost independent on temperature. Furthermore, the GB diffusion is strongly dependent on its structure and the interfacial potential energy. The lower oxygen-to-metal (O/M) ratio gives the larger GB diffusion coefficients for actinides and oxygen.

KEYWORDS: molecular dynamics simulation, oxide fuel, actinide, diffusion, grain boundary

I. Introduction

Recently, to reduce the environmental burden and to use the repository efficiently, the partitioning and transmutation of minor actinides (MAs) is an option for the future nuclear fuel cycle. Hence, various MA-containing fuels garner attention as advanced nuclear fuels for fast reactors or transmutation systems.

Americium is the key element of the MAs, and especially, Am-241 (half-life 433 years) and Am-243 (half-life 7,380 years) are the most important ones on resolving the above issues. As is well known, a lot of studies of uranium (or plutonium) oxides and their solid solutions used as nuclear fuel materials have been performed for the thermal and mechanical properties so far.¹⁻¹⁶⁾ However, there are relatively few studies of americium oxides. This is caused by its radio-toxicity and chemical instability. For instance, americium dioxide and Am-including oxides are easily reduced in high temperatures. As a result, the O/M ratio could change during the measurement.

Diffusion behaviors of actinides and oxygen in fuels are directly or indirectly relating to various physico-chemical properties, e.g. actinide and oxygen redistribution, pore migration, burn-up distribution, etc. Recently, we have evaluated the Pu and Am diffusion behaviors in Am-MOX (americium-including mixed oxide) fuels experimentally.¹⁷⁾ That study showed that the diffusion coefficients of Pu and Am were almost comparable with that of U, and their GB

diffusion was much larger than bulk ones. In addition, the lower oxygen potential increased their diffusion coefficients.

On the other hand, we have developed the MD simulation technique in order to investigate the thermo-chemical properties of oxide fuels, e.g. thermal conductivity, heat capacity, diffusion behaviors. The MD study can reveal the atomistic behavior for macroscopic (or experimental) phenomena and does not need a special facility to handle the radioactive materials. Our previous study of UO₂ using the MD simulation showed that the O diffusion mechanism changes as a temperature increased: the diffusion via its vacancies and with the formation of Frenkel defects and the superionic conduction; the U ion diffused only via its vacancies.¹⁸⁾ In addition, the GB diffusion was significantly larger than bulk one, and the GB diffusion coefficient strongly depended on its structure.

Hence, in this study, we investigated the diffusion behaviors in GBs for constituent ions of americium dioxide and Am-including uranium oxides from the point of views of temperature, GB structure and the O/M ratio dependence.

II. Simulation Method

MD simulations were performed by the MXDORTO program parallelized with Message Passing Interface (MPI) and its original program was coded by Kawamura.¹⁹⁾ Since the supercell including GBs was relatively large and consisted of max. 28,000 particles, the MPI parallelized MD program was used. In the MD calculation, the interatomic potential function for oxide fuels was the Born-Mayer type with a

*Corresponding author, E-mail: nishina@nucl.kyushu-u.ac.jp

partially ionic valence. This potential function is given by

$$U_{ij}(r_{ij}) = \frac{z_i z_j e^2}{r_{ij}} + f_0(b_i + b_j) \exp\left(\frac{a_i + a_j - r_{ij}}{b_i + b_j}\right) - \frac{c_i c_j}{r_{ij}^6} \quad (1)$$

where z_i is 67.5% of the formal charge of type i ion, e the electron charge, r_{ij} the distance between ions of i and j , f_0 the adjustable parameter. Potential parameters, a , b and c are the characteristic parameters depending on ion species. These potential parameters for the oxygen ion were given by Inaba²⁰⁾ and the parameters for actinide ions were determined by our previous studies.^{18,21)}

In this study, the GB structures of $\Sigma 41$, $\Sigma 13$, $\Sigma 5$ and $\Sigma 2$ were explored. These GB structures were constructed based on the coincidence-site-lattice (CSL) theory for the fluorite crystal structure,²²⁾ and have misorientation angles of 12.7°, 22.6°, 36.9° and 46.4°, respectively. For instance, the supercell including $\Sigma 5$ GBs is shown in **Fig. 1**.

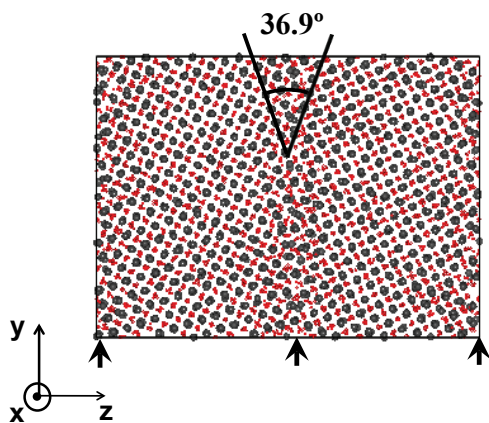


Fig. 1 Supercell including $\Sigma 5$ GBs with the misorientation angle of 36.9°. GB interfaces are shown by small arrows and are parallel to the x-y plane. Large black balls and small red ones stand for actinide and oxygen ions, respectively.

The self-diffusion coefficient of each atoms is determined based on the time evolution of the mean square displacements (MSD). This quantity can be easily determined by recording the atomic positions regularly during the simulation. The MSD function at time t corresponds to the average square distance travelled by an atom between t_0 and t . It is calculated with the following equation:

$$\text{MSD} = \langle |r_i(t) - r_i(t_0)|^2 \rangle \quad (2)$$

where $r_i(t_0)$ is the position of the atom i at the initial time t_0 , and $r_i(t)$ the position at the time t . The three-dimensional diffusion coefficients, D , are deduced from the MSD functions using the Einstein's relation expressed in Eq. (3). In order to obtain the reliable diffusion coefficient, the larger time steps are required for the MD calculation. Thus, total time steps for one run are 5×10^5 steps (1 step = 2 fs), and 5×10^3 steps, which correspond to infinite t in Eq. (3), are used to determine the diffusion coefficient from the asymptotic slope of the MSD function (**Fig. 2**). In Fig. 2, the MSD

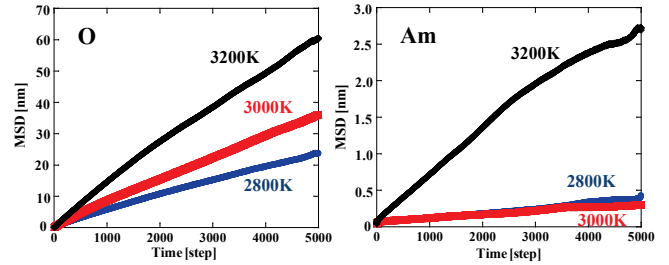


Fig. 2 E MSD functions of O and Am ions in $\Sigma 5$ GB

functions of Am at 2,800 K and 3,000 K are almost same and it probably seems strange. As discussed later, $\Sigma 5$ GB structure is possible to be relatively stable at lower temperatures. So, the MSD functions of cations become smaller with decreasing temperature, and the jump frequency is very low, which causes the increase of the statistical error.

$$D = \lim_{t \rightarrow \infty} \frac{1}{6t} \langle |r_i(t) - r_i(t_0)|^2 \rangle \quad (3)$$

In general, diffusion in solid occurs with point defects. The point defect concentration is thermally activated, and it increases with an increase of temperature. Migration is also a thermally activated process, accelerated with increasing temperatures. The diffusion coefficient can then be written as follows:

$$D = D_0 \exp\left(-\frac{Q}{k_B T}\right) \quad (4)$$

where Q is the sum of the defect formation energy and the migration energy of the defect, D_0 a pre-exponential factor independent of the temperature, k_B the Boltzmann constant, and T the temperature. For GBs, the activation energy calculated from the slope of an Arrhenius diagram ($\ln D$ as a function of $1/T$) is equivalent to the migration energy, because the point defect formation energy which regulates the point defects concentration is not included in the calculation of the diffusion activation energy.

III. Results and Discussion

1. GB Diffusion Coefficient versus Temperature

To investigate the influence of GB on diffusion coefficients, the simulation box was divided into 0.6 nm width slabs along the z-axis parallel to the GB interface. Firstly, particles existing in each slab at a final state were identified, and subsequently their trajectories were traced. This allows these particles to diffuse longer than 0.6 nm in the z-direction. Finally, diffusion coefficients were calculated with the MSD functions, Eq. (3), for these particle in each slab.

GB diffusion coefficients were calculated for the slab including the GB interface as a function of temperature. The temperature range was from 2,600 K to 3,400 K. This target temperature, 3,400 K, is somewhat higher than the experimental melting point of UO_2 , 3,120 K. There are two reasons: (1) for lower temperatures, the jump frequency is

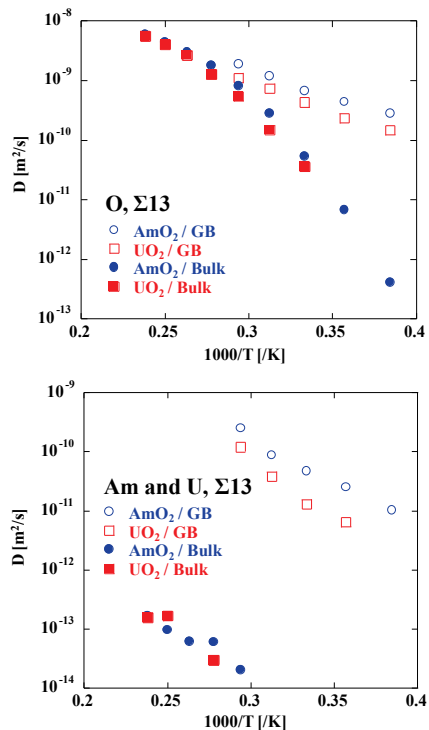


Fig. 3 Diffusion coefficients of oxygen and actinides

extremely low and the diffusion coefficients of cations cannot be obtained since the calculated melting point is 3,675 K,²³⁾ (2) the diffusion mechanism will not change even for such higher temperatures. The results obtained for the Σ13 GB structure are shown in **Fig. 3**. For comparison, the bulk diffusion coefficients are also plotted in this figure. Here, the bulk diffusion coefficients were calculated for the supercell including neither point defects nor GBs. As shown in this figure, the O diffusion coefficients for the Σ13 GB are higher than bulk ones. In addition, the slope, i.e. activation energy, of Arrhenius plot for oxygen diffusion in GBs is almost same as that in the bulk at high temperatures. So, oxygen ions in GBs diffuse in a state of the superionic conduction, because oxygen ions in the bulk diffuse in the same way, which shown in our previous study.¹⁸⁾ On the other hand, the GB diffusion coefficients of Am and U ions are significantly ($\sim 10^4$ times) larger than bulk ones. Especially for actinide ions, their diffusions were accelerated in the GB region.

2. Diffusion Coefficient Evolution with Distance from GB Interface

To evaluate the diffusion coefficient as a function of the distance from the GB interface, we calculate them at 3,200 K for Σ5 GB in AmO₂. The results are shown in **Fig. 4**. For comparison, the bulk oxygen diffusion coefficients obtained from AmO₂ perfect crystal are also plotted in Fig. 4. Meanwhile, the bulk diffusion coefficient of americium is not plotted because it depends on the number of lattice defects, e.g. Schottky defect, and the temperature is too low.

In **Fig. 4**, the influence of the GB on the oxygen diffusion can be found from GB interface to approximately 3 nm. In

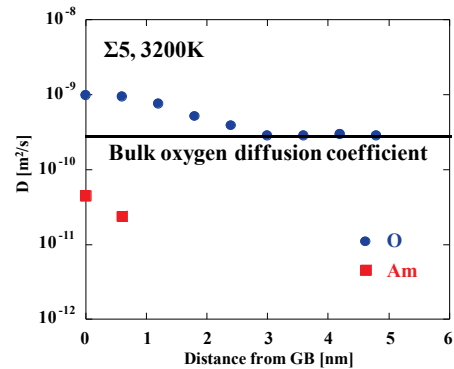


Fig. 4 Influence of GB on the oxygen diffusion coefficient as a function of the distance from the GB interface. The line shows the bulk diffusion coefficient obtained for AmO₂ perfect crystal

the region over 3 nm, the oxygen diffusion coefficients are nearly equal to those calculated in the bulk. The same analysis for UO₂ was performed by Aublant *et al.*²⁴⁾ Their result shows that the diffusion coefficients of oxygen far from the GB interface are much lower than those near the GB, but their values are larger than bulk one. This result differs from our results, which may be originated from the potential function. Their potential function is proposed by Morelon *et al.*²⁵⁾ and seems to give the relatively larger diffusion coefficients of O and U. As a result, the effect of the GB may be significant. On the contrary, our potential function seems to give smaller oxygen diffusion coefficient in comparison with other potential functions.²⁶⁾ Hence, for our result, the GB has little effect on the oxygen diffusion coefficients far from GB interface.

On the other hand, the influence of the GB on the americium diffusion can be found only narrow region (approx. 1 nm), and Am diffusion coefficients for Σ5 GB are much smaller than those of oxygen. In the region over 1 nm, the Am diffusion coefficient was too small to evaluate.

Furthermore, in order to evaluate the effect of interference between GBs, we calculated the diffusion coefficients for the large supercell (about double-wide to the z-axis) for the Σ5 GB structure. As a result, we confirmed that there was no difference between diffusion coefficients obtained for the normal supercell and large one.

3. Misorientation Angle Dependence of GB Diffusion

In order to study the misorientation angle dependence of GB diffusion, we calculate the diffusion coefficients for the GBs of Σ41, Σ13, Σ5 and Σ29 as a function of temperature. The results are shown in **Fig. 5**. The graphs show that the diffusion coefficients of O and Am increase with an increase of the misorientation angle. In addition, the slope of the Arrhenius plot for oxygen becomes lower as an increase of misorientation angle and the values are almost same at higher temperatures. This means that the effect of GB structure becomes smaller with increasing temperature, that is the disappearance of the crystalline nature of GBs. On the other hand, americium shows the almost same tendency as oxygen except for the Σ5 GB structure. Especially for lower temperatures, the GB diffusion coefficient for Σ5 structure seems to

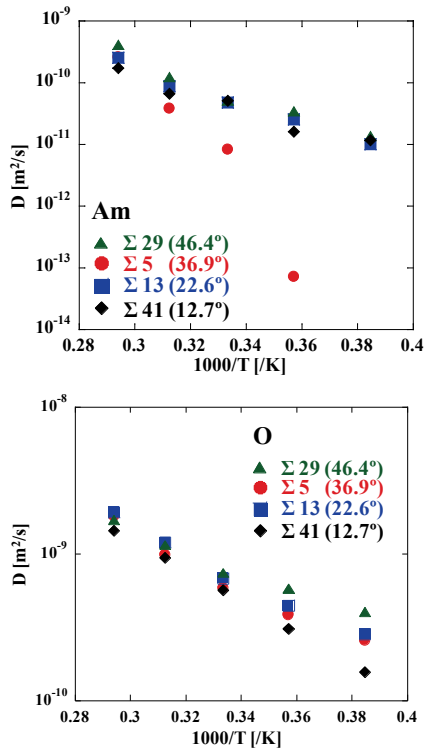


Fig. 5 Misorientation angle dependence of GB diffusion coefficients

be small, and its Arrhenius relation has a steeper slope.

So, we calculated the interfacial potential energy of each GB structure. Here, the definition of the GB potential energy is given by

$$E_{\text{GB potential}} = \frac{E_{\text{GB supercell}} - E_{\text{Perfect supercell}}}{2A} \quad (5)$$

where $E_{\text{GB supercell}}$ is the total potential energy of the supercell including GBs, $E_{\text{Perfect supercell}}$ is that of perfect crystal, A is the area of the GB interface. Since each GB supercell is including two GB interfaces in it, the denominator is multiplied by 2. The results are plotted in **Fig. 6**. This graph shows that the GB potential energy almost increases as an increase of the misorientation angle, but slightly decreases at the misorientation angle of $\Sigma 5$ GB. This may be interpreted as the stability of $\Sigma 5$ GB structure, which results in the smaller diffusion coefficient of Am in $\Sigma 5$ GB.

Figure 7 shows Am ion trajectories in GBs. The $\Sigma 41$ and $\Sigma 13$ GBs have smaller misorientation angle and the trajectories seem to be one dimensional and parallel to the x-axis. Whereas, in the $\Sigma 29$ GB with the large misorientation angle, the trajectory seems to be two dimensional or planar and parallel to the x-y plane.

4. O/M Ratio Dependence of GB Diffusion

To study the O/M ratio dependence of diffusion in the GB, we calculated the diffusion coefficients for the supercell of the solid solution substituted $\text{AmO}_{1.5}$ for 20 mol% of UO_2 . Here, all additive Am ions are trivalent, consequently the O/M ratio of the solid solution is 1.9. In addition, to improve

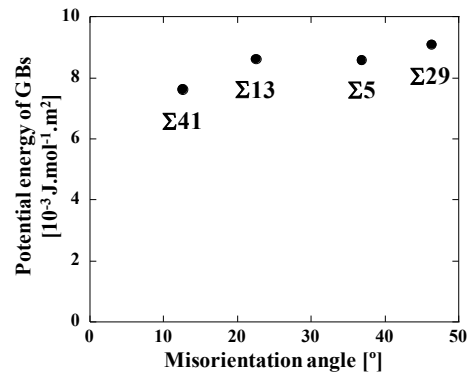


Fig. 6 GB potential energy as a function of misorientation angle. These values were calculated at 300 K.

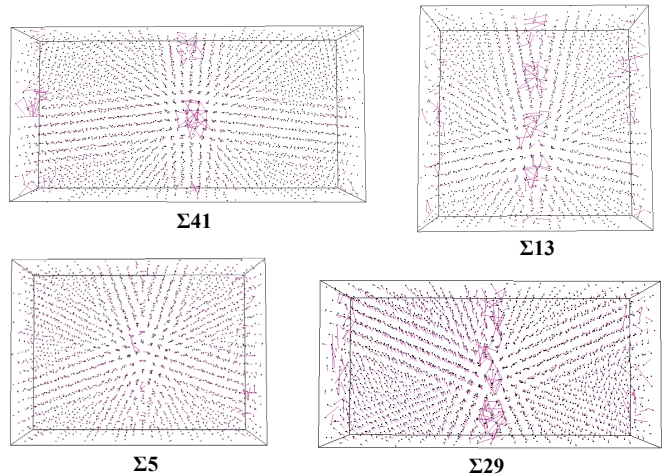


Fig. 7 Am trajectories in GBs at 3,000 K. The xyz coordination system is same as that of Fig. 1.

the statistical reliability for the trivalent Am ion, the diffusion coefficients of constituent ions were calculated for the large supercells (about double-wide to the y-axis).

The results are shown in **Fig. 8**. For comparison, the diffusion coefficients of U and Am for the O/M=2.0 are calculated for the GB in UO_2 and AmO_2 supercells, respectively. As shown in these graphs, the diffusion coefficients of U and Am increase as the decrease of the O/M ratio. To clarify the O/M effect on GB diffusion, we calculated the pair correlation functions (PCFs) in AmO_2 and $(\text{U}, \text{Am}^{3+})\text{O}_{1.9}$ from the viewpoint of the local lattice structure. **Figure 9** shows that distances of O-O and Am-O are extended by substituting $\text{AmO}_{1.5}$ for 20mol% of UO_2 . Since cations are surrounded by oxygen ions even in grain boundaries, cations must diffuse out of the cage consisting of O ions. Therefore, not only Am^{3+} ion, but also U ion more easily migrates into the nearest vacant site because of the increase of the distance between O-O. Furthermore, the binding energy between Am^{3+} -O ions is smaller than that of tetravalent cation-O ion since the Coulomb energy of the former is small. Thus, it also causes the increase of GB diffusion coefficient of Am^{3+} ion.

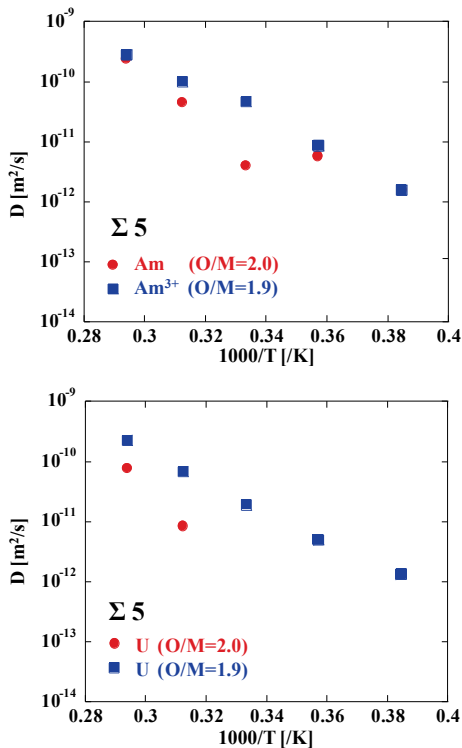


Fig. 8 O/M ratio dependence of diffusion coefficients of U and Am ions for $\Sigma 5$ GB structure

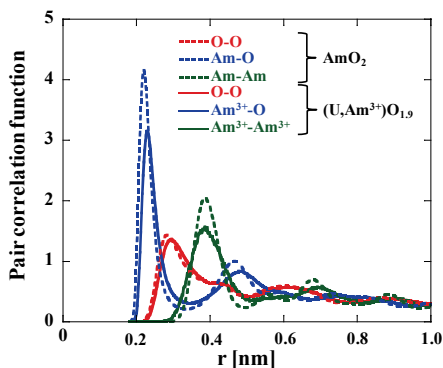


Fig. 9 Pair correlation functions of O-O, Am-O and Am-Am. Solid and dashed lines show PCFs in AmO_2 and $(\text{U}, \text{Am}^{3+})\text{O}_{1.9}$, respectively.

IV. Conclusion

The MD simulations have been carried out to study actinide and oxygen diffusion near symmetrical tilt grain boundaries $\Sigma 41$, $\Sigma 13$, $\Sigma 5$ and $\Sigma 29$.

It has been observed an acceleration of the diffusion near GB for both actinide and oxygen ions. Concerning the O diffusion mechanism, O ions in the GBs diffuse in a state of the superionic conduction. In addition, the GB has the influence on the O diffusion at the farther distance from the GB interface.

The diffusion coefficients of O and Am ions increase as an increase of the misorientation angle of GB. From the results of the interfacial potential energies of GBs, the Σ GB structure is stable compared with others.

The GB diffusion coefficients of U and Am increase as the decrease of the O/M ratio. This may be because the distance between O ions surrounding cations increases by the addition of Am^{3+} and by the increase of the number of O vacancies. In addition, the decrease of the binding energy between Am^{3+} -O ions causes the increase of its GB diffusion coefficient.

References

- 1) A. B. Auskern, J. Belle, "Uranium ion self-diffusion in UO_2 ," *J. Nucl. Mater.*, **3**, 311-319 (1961).
- 2) F. Schmitz, R. Lindner, "Diffusion of heavy elements in nuclear fuels: actinides in UO_2 ," *J. Nucl. Mater.*, **17**, 259-269 (1965).
- 3) S. Yajima, H. Furuya, T. Hirai, "Lattice and grain-boundary diffusion of uranium in UO_2 ," *J. Nucl. Mater.*, **20**, 162-170 (1966).
- 4) R. J. Hawkins, C. B. Alcock, "A study of cation diffusion in UO_{2+x} and ThO_2 using α -ray spectrometry," *J. Nucl. Mater.*, **26**, 112-122 (1968).
- 5) J. F. Marin, P. Contamin, "Uranium and oxygen self-diffusion in UO_2 ," *J. Nucl. Mater.*, **30**, 16-25 (1969).
- 6) Hj. Matzke, "On uranium self-diffusion in UO_2 and UO_{2+x} ," *J. Nucl. Mater.*, **30**, 26-35 (1969).
- 7) Hj. Matzke, "Diffusion of Th and U in thorium dioxide," *J. Phys.*, C7[12], 452-457 (1976).
- 8) A. C. S. Sabioni, W. B. Feraz, F. Millot, "First study of uranium self-diffusion in UO_2 by SIMS," *J. Nucl. Mater.*, **257**, 180-184 (1998).
- 9) G. L. Reynolds, "The surface self-diffusion of uranium dioxide," *J. Nucl. Mater.*, **24**, 69-73 (1967).
- 10) M. O. Marlowe, A. I. Kaznoff, "Tracer study of the surface diffusivity of UO_2 ," *J. Nucl. Mater.*, **25**, 328-333 (1968).
- 11) E. N. Hodkin, M. G. Nicholas, "Surface and interfacial properties of stoichiometric uranium dioxide," *J. Nucl. Mater.*, **47**, 23-30 (1973).
- 12) E. N. Hodkin, M. G. Nicholas, "Surface and interfacial properties of non-stoichiometric uranium dioxide," *J. Nucl. Mater.*, **67**, 171-180 (1977).
- 13) G. L. Reynolds, B. Burton, "Grain-boundary diffusion in uranium dioxide: the correlation between sintering and creep and a reinterpretation of creep mechanism," *J. Nucl. Mater.*, **82**, 22-25 (1979).
- 14) A. C. S. Sabioni, W. B. Feraz, F. Millot, "Effect of grain-boundaries on uranium and oxygen diffusion in polycrystalline UO_2 ," *J. Nucl. Mater.*, **278**, 364-369 (2000).
- 15) G. Riemer, H. L. Scherff, "Plutonium diffusion in hyperstoichiometric mixed uranium-plutonium dioxides," *J. Nucl. Mater.*, **39**, 183-188 (1971).
- 16) Hj. Matzke, "Diffusion processes and surface effects in non-stoichiometric nuclear fuel oxides UO_{2+x} and $(\text{U}, \text{Pu})\text{O}_{2\pm x}$," *J. Nucl. Mater.*, **114**, 121-135 (1983).
- 17) I. Sato, K. Tanaka, T. Arima, "Diffusion behaviors of plutonium and americium in polycrystalline urania," *IOP Conf. Ser. Mat. Sci. Eng.*, **9**, 012005 (2010).
- 18) T. Arima, K. Yoshida, K. Idemitsu, Y. Inagaki, I. Sato, "Molecular dynamics analysis of diffusion of uranium and oxygen ions in uranium dioxide," *IOP Conf. Ser. Mat. Sci. Eng.*, **9**, 01203 (2010).
- 19) Kawamura, <http://www.geo.titech.ac.jp/lab/kawamura/>
- 20) H. Hayashi, R. Sagawa, H. Inaba, K. Kawamura, "Molecular dynamics calculations on ceria-based solid electrolytes with

- different radius dopants,” *Solid State Ionics*, **131**, 281-290 (2000).
- 21) T. Uchida, T. Arima, K. Idemitsu, Y. Inagaki, “Thermal conductivities of americium dioxide and sesquioxide by molecular dynamics simulations,” *Comput. Mater. Sci.*, **45**, 229-234 (2009).
- 22) H. Ogawa, “GBstudio: a builder software on periodic models of CSL boundaries for molecular simulation,” *Mat. Trans.*, **47**, 2706-2710 (2006).
- 23) T. Arima, K. Idemitsu, Y. Inagaki, Y. Tsujita, M. Kinoshita, E. Yakub, “Evaluation of melting point of UO₂ by molecular dynamics simulation,” *J. Nucl. Mater.*, **389**, 149-154 (2009).
- 24) E. Vincent-Aublant, J-M. Delaye, L. Van Brutzel, “Self-diffusion near symmetrical tilt grain boundaries in UO₂ matrix: A molecular dynamics simulation study,” *J. Nucl. Mater.*, **392**, 114-120 (2009).
- 25) N. D. Morelon, D. Ghaleb, J. M. Delaye, L. Van Brutzel, “A new empirical potential for simulating the formation of defects and their mobility in uranium dioxide,” *Phil. Mag.*, **83**, 1533-1550 (2003).
- 26) K. Govers, S. Lemehov, M. Hou, M. Verwerft, “Comparison of interatomic potentials for UO₂ Part II: Molecular dynamics simulations,” *J. Nucl. Mater.*, **376**, 66-77 (2008).
-